Environmental Science and Pollution Research (2020) 27:15984–15993
https://doi.org/10.1007/s11356-019-05189-9

SEDIMENT RESEARCH AND MANAGEMENT

Phosphorus recovery by ion exchange in a solid carbonate: modeling of the process

Luis A. Cueto[1] · Anne M. Hansen[2]

Received: 31 October 2018 / Accepted: 15 April 2019 / Published online: 4 May 2019

Abstract

Phosphorus (P) is a nutrient for plant growth but also a pollutant in water bodies causing eutrophication. The source of P is mainly human and animal wastewater and runoffs from different land uses. The objective of the present study is to evaluate P removal and recovery processes by ion exchange (IE) with solid carbonate (SC) in biodigestor-treated swine effluent (BTSE) using hydrogeochemical modeling. For this, BTSE compositions were obtained by literature review. A synthetized and characterized SC was used and the ion exchange site concentration ([SC-IE]) and the IE constants (K_{ie}) were obtained experimentally and applied to model P and major anion removal and recovery processes. P recovery was evaluated for different BTSE compositions and several concentrations of SC, dissolved P (HPO_4^{2-}), competing anions such as SO_4^{2-}, and CO_3^{2-}. The simulations suggest that a [SC-IE]:[HPO_4] of 1.4 molar ratio would allow the recovery of 90% of HPO_4 in BTSE, and at average alkalinity concentrations in BTSE, CO_3^{2-} would compete with HPO_4 for the SC-IE. The P recovery by the SC-IE process was compared with two other methods commonly used in P removal from BTSE: removal with aluminum sulfate and precipitation of struvite as a function of pH. The results suggest that SC-IE is the most efficient method in the pH range of BTSE. Besides, HPO_4^{2-} was readily recovered as inorganic P that may be reused in agriculture and industrial processes.

Keywords Biodigestor-treated swine effluent · Modeling with PhreeqC · Eutrophication control · Equilibrium constants · Competing anions

Introduction

The eutrophication is a form of water pollution caused by accumulation of nutrients, mainly nitrogen (N) and phosphorous (P). Generally, nutrients are emitted from point and diffuse sources in watersheds and are readily mobilized to water and sediments in rivers, lakes, and reservoirs.

Although nutrient emissions from different sources may comply with maximum allowable concentrations in diverse environmental regulations, nutrient loads to water bodies depend not only on the concentrations but also on the discharged fluxes. Nutrient loads to water bodies also depend on the way the nutrients are emitted, mobilized, and attenuated in water, sediment, and vegetation in river basins. Since nutrient emissions from livestock discharges may represent important emissions in hydrologic basins (Jayme-Torres and Hansen 2018), to control the eutrophication in water bodies, it is necessary to control emissions from these sources.

Among nutrients that produce eutrophication in water bodies, P is commonly found in limiting concentrations for plant growth, so that its removal from the source may control eutrophication (Xu et al. 2014). Besides, P is a non-renewable resource, and according to Cordell et al. (2011), the known supplies of this nutrient would be exhausted in approximately three decades. It is therefore urgent to develop methods that allow recovering and recycling P, which is currently discharged from productive activities, contaminating water bodies. Among the principal sources of such wasted P is livestock farming, and it is estimated that about 40% of total produced P is discharged as livestock waste that pollutes water bodies (Rittmann et al. 2011). Livestock farming waste has

Responsible editor: Philippe Garrigues

✉ Anne M. Hansen
ahansen@tlaloc.imta.mx

[1] Programa de Maestría y Doctorado en Ingeniería, Universidad Nacional Autónoma de México, Campus Instituto Mexicano de Tecnología del Agua, Jiutepec, Morelos, Mexico

[2] Instituto Mexicano de Tecnología del Agua, Paseo Cuauhnáhuac 8532, 62550 Jiutepec, Morelos, Mexico

relatively low fluxes and elevated concentrations of P in comparison to other sources such as domestic and municipal wastewater that is usually diluted with graywater and rainwater, making the nutrient's recovery more difficult. The condition of elevated P concentrations and low fluxes benefits the P recovery process as compared to conditions of higher fluxes and low concentrations.

Swine emissions are also characterized by high concentrations of suspended solids (SS), organic matter (OM), and other nutrients (Ye et al. 2011), and are typically treated to remove SS and OM before discharge. Actually, the most common treatment of these emissions is anaerobic biodigestion, a system that takes advantage of the fermentation of OM by microorganisms in swine waste in the absence of oxygen. The process can reduce OM to acceptable regulation levels; also, it generates biogas that can be used in productive activities. The biodigestion treated swine effluent (BTSE) requires a post-biodigestor treatment in order to reduce the P concentrations (Rittmann et al. 2011). Some of the most common methods used for this post-biodigestor P removal from BTSE are precipitation of struvite (Suzuki et al. 2007; Ye et al. 2011), P retention in polyphosphate-accumulating organisms (PAO) (Rittmann et al. 2011), and P sorption or ion exchange (IE) in minerals and other materials (Yuan et al. 2015). It is a common practice to reuse stabilized wastes and sludge produced during fermentation of swine waste as fertilizers in soils; but in most cases, the transport costs restrict this practice (Cordell et al. 2011).

The P removal by precipitation of struvite and its reuse as slow-release fertilizer suggest that this method is a promising alternative for the reuse of P. However, the presence of cations such as Ca^{2+} and K^{+} and anions such as CO_3^{2-} and SO_4^{2-} may cause formation of other minerals, competing with the production of struvite (Ye et al. 2011). In addition, the struvite precipitation process requires values of pH higher than 9, so it is necessary to increase the pH of the BTSE by adding alkali in the process.

The PAO can remove P as biomass in anaerobic-aerobic cycles. This process is especially efficient for high concentrations of P present in BTSE. Although the produced biomass can be used directly as fertilizer, the process had a high energy cost and can require additional treatments for reuse and recovery of removed P (Rittmann et al. 2011).

The P removal methods based on sorption include the use of minerals such as dolomite and bentonite or industrial subproducts such as fly ash or steel slag. In some cases, the removed P can be recovered for reuse. These methods are widely used mostly due to the low costs and the wide availability of the sorbents; however, the large fluxes of generated waste require large reactors, representing a disadvantage for its application (Cordell et al. 2011).

The IE for P removal has the advantage of being a reversible process, making recovery of P more achievable. Some of the IE methods reported for P removal and recovery are based on the use of metal-loaded resins, double-layered hydroxides, or minerals composed of carbonate such as hydrotalcite, dolomite, and calcite (Cordell et al. 2011). However, the presence of other anions as SO_4^{2-} and CO_3^{2-} in BTSE may reduce the efficiency of the IE processes and decrease the useful period of the ion exchanger.

In all these processes, pH, major solution ions, and organic functional groups in BTSE may affect the efficiencies of P removal and recovery and should therefore be addressed. We selected ion exchange for evaluation of the removal of P in BTSE because in principle this method allows more convenient recovery of P. The objective of the present study is therefore to evaluate the P removal and recovery processes with a solid carbonate (SC) in BTSE using hydrogeochemical modeling.

Methods

The BTSE solution chemistry was obtained by literature review and a synthetized and characterized the ion exchange site concentrations on SC [SC-IE] and the ion exchange equilibrium constants (K_{IE}) were obtained and the P removal and recovery processes on SC were evaluated.

Solution chemistry of biodigestor-treated swine effluent

Average values and standard deviations of ion concentrations, pH, pe, and chemical oxygen demand (COD) from BTSE were obtained from literature search (Table 1). COD was converted to concentration of acetate as the simplest organic compound contained in the Thermoddem database (Blanc 2017).

Modeling of phosphorus removal and recovery from solid carbonate

The PHREEQC v. 3.4.6 (USGS, Middleton, USA) (Parkhurst and Appelo 2013) and the thermodynamic data reported in the Thermoddem database developed by BRGM (Bureau de Recherches Géologiques et Minières) (Blanc 2017) were used to model the speciation of aqueous components in BTSE and their interaction with SC. This database was selected because it describes most of the reactions of dissolved P as well as saturation indexes of solid P phases. Other reactions were obtained from the LLNL database (LLNL, Livermore, USA 2010); Wagman et al. (1982) or calculated based on $\Delta G°$ values (Drever 1982). All reactions are presented in Table 2 and included in the Thermoddem database or as modeling input data. The modified Davies equation was used for ion activity coefficient calculations at ionic strengths below 0.5 M and the Pitzer equation was used for ionic strengths above 0.5 M.

Table 1 Composition of biodigestor-treated swine effluent

Parameter	Average	SD (*n*)	Scenario evaluation with PHREEQC (Y/N)
pH[a,b,c,d,e]	7.3	0.6 (5)	Y
pe	− 4.2	N/A	N
Total N (mg l^{-1})[a,b,c,d,e]	1888	1566 (5)	N
N-NO_3 (mg l^{-1})[a,e,f,g,h]	23	19 (5)	N
NH_4 (mg l^{-1})[a,b,c,d,e]	1344	1335 (5)	N
Total P (mg l^{-1})[a,b,c,d,e]	351	174 (5)	N
P-PO_4 (mg l^{-1})[b,d,f,g,h]	115	88 (5)	Y
Cl (mg l^{-1})[e,f,i]	1355	1663 (3)	N
SO_4 (mg l^{-1})[a,f,h]	182	180 (3)	Y
Alkalinity (mg-$CaCO_3$ l^{-1})[c]	5590	N/A (1)	Y
Ca (mg l^{-1})[e,f,i]	91	53 (3)	Y
Mg (mg l^{-1})[e,f,i]	72	18 (3)	Y
Na (mg l^{-1})[e,f,i]	831	692 (3)	N
K (mg l^{-1})[b,e,i]	2585	2526 (3)	N
Fe (mg l^{-1})[e,f,i]	31	15 (3)	Y
COD (mg l^{-1})[a, b,d,e]	4663	300 (4)	N
Total SS (mg l^{-1})[a,b,c,d]	5783|	8670 (4)	N

[a] Martin 2003
[b] Cheng et al. 2003
[c] Rodríguez and Lomas 1999
[d] Ra et al. 2000
[e] Meers et al. 2006
[f] Ye et al. 2011
[g] Mehta and Batstone 2013
[h] Bergland et al. 2015
[i] Barker and Overcash 2007

Determination of equilibrium constants and ion exchange site concentrations

A synthetized and characterized SC (Cueto and Hansen 2017) was used, [SC-IE] and K_{IE} for major anions on the SC were obtained experimentally and the results were described by independent modeling with PHREEQC to validate the modeled results.

The IE on SC were evaluated for dissolved P (HPO_4^{2-}), the major anions: Cl^-, NO_3^-, and SO_4^{2}, as well as CH_3COO^- for different concentrations of SC (1–6 g l^{-1}) suspended in 30 ml 0.1 M KCl as background electrolyte (KNO_3 was used as background electrolyte for the experiment with Cl^-) in 50-ml closed reactors. Reactors were agitated at 60 rpm in rotated mixers at room temperature of 25 ± 2 °C. A parallel control experiment was carried out without SC to assure that anions were not adsorbed on the reactor walls. Before adding the study anions, reactors were equilibrated until constant pH during approximately 30 min and 10-ml aliquots of 4 mM salts of the evaluated anions were then added to obtain 1 mM final concentrations of KCl, KNO_3, K_2SO_4, $C_2H_5O_2Na$, or K_2HPO_4 (JT Baker, ACS grade, Phillipsburg, USA). Anion concentrations and pH were monitored until equilibrium was reached in approximately 48 h. To measure anion concentrations, 1 ml supernatant aliquots were obtained and filtered through a 0.45-μm Millipore® membrane (Merck, Darmstaldt, GE) and the anions were measured by analytic tests Spectroquant® for phosphate (#100474, Merck), nitrate (#109713, Merck), chloride (#114897, Merck), sulfate (#100617, Merck), and total organic carbon (#114878, Merck). These anions were measured spectrophotometrically (Pharo 300, Merck, Darmstadt, GE) and carbonate was measured at the end of the experiment in 10 ml acidified samples (pH < 5) using an ion selective electrode for CO_2 (Hanna, Limena, IT). All assays were conducted in triplicate and experimental results were corrected for extracted volumes.

To obtain K_{ie} and [SC-IE], equilibrium data for different SC concentrations were analyzed using a linearization of the Langmuir isotherm according to van den Berg and Kramer (1979). [SC-IE] was calculated based on the surface area for SC of 13.5 g m^{-2} reported by Cueto and Hansen (2017).

Table 2 Reactions describing interactions of ions and solid-phase formation in biodigestor-treated swine effluent

Reaction	Equation	Log K
Solubility of SC	$SC \rightleftarrows Cat^{2+} + CO_3^{2-}$	8.6[a]
P removal with $Al_2(SO_4)_3$	$Al_2(SO_4)_3 + 6H_2O \rightleftarrows 2Al(OH)_3 + 2SO_4^{2-} + 6H^+$	0.4[b]
	$Al(OH)_3 + 3H^+ \rightleftarrows Al^{3+} + 3H_2O$	7.3[c]
	$HPO_4^{2-} + Al^{3+} \rightleftarrows AlPO_4(s) + H^+$	1.2[c]
Precipitation of struvite	$Mg^{2+} + NH_4^+ + PO_4^{3-} + 6H_2O \rightleftarrows MgNH_4PO_4{\cdot}6H_2O$	13.2[d]
Proton exchange	$H_2CO_3 \rightleftarrows HCO_3^+ + H^+$	− 6.3[c]
	$HCO_3^- \rightleftarrows CO_3^{2-} + H^+$	− 10.3[c]
	$H_3PO_4 \rightleftarrows H_2PO_4^- + H^+$	− 2.1[c]
	$H_2PO_4^- \rightleftarrows HPO_4^{2-} + H^+$	−7.2[c]
	$HPO_4^{2-} \rightleftarrows PO_4^{3-} + H^+$	− 12.4[c]
	$HSO_4^- \rightleftarrows SO_4^{2-} + H^+$	− 2.0[c]
	$HNO_3 \rightleftarrows NO_3^- + H^+$	− 1.3[c]
	$CH_3COOH \rightleftarrows CH_3COO^- + H^+$	− 4.8[e]
Ion pair formations	$Ca^{2+} + HCO_3^- \rightleftarrows CaCO_3 + H^+$	− 7.1[c]
	$Ca^{2+} + HCO_3^- \rightleftarrows CaHCO_3^+$	1.1[e]
	$Ca^{2+} + PO_4^{3-} \rightleftarrows CaPO_4^-$	6.5[c]
	$Ca^{2+} + H_2PO_4^- \rightleftarrows CaH_2PO_4^+$	1.4[f]
	$Ca^{2+} + HPO_4^{2-} \rightleftarrows CaHPO_4$	2.7[f]
	$Ca^{2+} + SO_4^{2-} \rightleftarrows CaSO_4$	− 4.4[c]
	$Ca^{2+} + 2Cl^- \rightleftarrows CaCl_2$	− 1.3[c]
	$Ca^{2+} + 2NO_3^- \rightleftarrows Ca(NO_3)_2$	1.0[c]
	$Ca^{2+} + CH_3COO^- \rightleftarrows CaCH_3COO^+$	− 3.8[e]
	$Fe^{3+} + H_2PO_4^- \rightleftarrows FeH_2PO_4^{2+}$	5.4[c]
	$Fe^{3+} + HPO_4^{2-} \rightleftarrows FeHPO_4^+$	5.4[c]
	$2Fe^{3+} + 3SO_4^{2-} \rightleftarrows Fe_2(SO_4)_3$	0.04[c]
	$Fe^{3+} + 2Cl^- \rightleftarrows FeCl_2$	1.5[c]
	$Fe^{3+} + NO_3^- \rightleftarrows FeNO_3^{2+}$	4.5[e]
	$Fe^{3+} + CH_3COO^- \rightleftarrows FeCH_3COO^{2+}$	− 3.5[e]
	$Mg^{2+} + PO_4^{3-} \rightleftarrows MgPO_4^-$	6.6[c]
	$Mg^{2+} + H_2PO_4^- \rightleftarrows MgH_2PO_4^+$	1.5[c]
	$Mg^{2+} + HPO_4^{2-} \rightleftarrows MgHPO_4$	− 4.3[f]
	$Mg^{2+} + SO_4^{2-} \rightleftarrows MgSO_4$	2.2[c]
	$Mg^{2+} + 2Cl^- \rightleftarrows MgCl_2$	− 0.1[f]
	$Mg^{2+} + 2NO_3^- \rightleftarrows Mg(NO_3)_2$	0.8[f]
	$Mg^{2+} + CH_3COO^- \rightleftarrows MgCH_3COO^+$	− 3.5[e]
Redox reactions	$0.25O_2 + Fe^{2+} + H^+ \rightleftarrows Fe^{3+} + 0.5H_2O$	8.5[c]
	$H^+ + SO_4^{2-} \rightleftarrows HS^- + 2O_2$	3.5[c]
	$2O_2 + NH_3 \rightleftarrows NO_3^- + H^+ + H_2O$	62[c]
Solid-phase formation reactions		
Aragonite	$HCO_3^- + Ca^{2+} \rightleftarrows CaCO_3(s) + H^+$	− 2.0[c]
$Ca_4H(PO_4)_3{:}2.5H_2O$.	$4Ca^{2+} + 3H_2PO_4^- + 2.5H_2O \rightleftarrows Ca_4H(PO_4)_3{\cdot}2.5H_2O(s) + 5H^+$	11.8[c]
Dolomite	$2HCO_3^- + Ca^{2+} + Mg^{2+} \rightleftarrows CaMg(CO_3)_2(s) + 2H^+$	3.5[c]
Mackinawite	$Fe^{2+} + HS^- \rightleftarrows FeS(s) + H^+$	− 3.5[c]
$FeSO_4$	$Fe^{2+} + SO_4^{2-} \rightleftarrows FeSO_4(s)$	1.1[c]
Hydroxyapatite	$5Ca^{2+}\ 3H_2PO_4^- + H_2O \rightleftarrows Ca_5(PO_4)_3(OH)(s) + 7H^+$	14.3[e]
Magnesite	$HCO_3^- + Mg^{2+} \rightleftarrows MgCO_3(s) + H^+$	1.4[c]
$MgHPO_4$	$Mg^{2+} + H_2PO_4^- \rightleftarrows MgHPO_4(s) + H^+$	− 5.8[c]
$MgSO_4$	$Mg^{2+} + SO_4^{2-} \rightleftarrows MgSO_4(s)$	9.1[c]
Monetite	$Ca^{2+} + H_2PO_4^- \rightleftarrows CaHPO_4(s) + H^+$	0.3[c]
Na_2HPO_4	$2Na^+ + H_2PO_4^- \rightleftarrows Na_2HPO_4(s) + H^+$	9.2[c]
Newberyte	$Mg^{2+} + H_2PO_4^- + 3H_2O \rightleftarrows MgHPO_4{\cdot}3H_2O(s) + H^+$	1.4[c]
Vivianite	$3Fe^{2+} + 2H_2PO_4^- + 8H_2O \rightleftarrows Fe_3(PO_4)_2{\cdot}8H_2O(s) + 4H^+$	−3.3[c]
Whitlockite	$3Ca^{2+} + 2\ H_2PO_4^- \rightleftarrows Ca_3(PO_4)_2(s) + 4H^+$	10.1[c]

[a] Based on ΔG values reported by Drever (1982)

[b] Wagman et al. (1982)

[c] Thermoddem database developed by the BRGM (Bureau de Recherches Géologiques et Minières) (Blanc 2017)

[d] Türker and Erdem (2011)

[e] LLNL database LLNL (Lawrence Livermore National Laboratory) (2010)

To evaluate the HPO_4^{2-} and SO_4^{2-} recovery, phosphate and sulfate-loaded SC were prepared by suspending known amounts of SC (from 1 to 6 g l^{-1}) in 40 ml 0.1 M KCl solutions with 1 mM K_2SO_4 or K_2HPO_4 during 72 h in 50-ml closed reactors. SC was separated by centrifugation and dried at 80 °C until constant weight. The recovered solids were added

to 40-ml solutions of 500 mM Na_2CO_3 (JT. Baker ACS grade) as eluent. After 48 h of equilibrations in rotated mixers at room temperature of 25 ± 2 °C. Supernatant aliquots were then obtained and phosphate or sulfate and carbonate were analyzed as previously described.

Model validation with experimental results

The ion removal and recovery experiments of HPO_4^{2-} and SO_4^{2-} were modeled by emulating the experimental conditions previously described. To validate the modeling results, ratios between modeled and experimental data were evaluated to describe the efficacy of the model to simulate the process.

Simulation of phosphorus removal and recovery in biodigestor-treated swine effluent

The removal and recovery of HPO_4^{2-} with SC in varying BTSE compositions were assessed by hydrogeochemical simulation with the validated model, and the effects of SC and different ion concentrations on these processes were analyzed. With this purpose, average, maximum, and minimum values for swine effluents were evaluated (Table 1). In addition, the recovery process with CO_3^{2-} as eluent was analyzed as a function of the ratio [SC-IE]:[HPO_4] molar ratio for different CO_3^{2} concentrations.

Comparison between phosphorus removal methods

Finally, P removal by SC-IE was compared with application of $Al_2(SO_4)_3$ and precipitation of struvite as a function of pH. The P removal processes were modeled using average BTSE concentrations (Table 1). The removal with $Al_2(SO_4)_3$ considered the P interactions with Al as presented in Table 2 and addition of equimolar concentration of the aluminum salt relative to P, according to a recommendation by Crittenden et al. (2012). The struvite precipitation was modeled considering the corresponding equations reported in Table 2 with [Mg]:[HPO_4] molar ratios of 1 and 6 as recommended by Ye et al. (2011). The P removal with SC-IE was modeled using [SC-IE]:[HPO_4] molar ratios of 0.8 and 1.4.

Results and discussion

Determination of equilibrium constants and ion exchange site concentrations

Results of experimental and calculated K_{IE} of HPO_4^{2} and competing anions (SO_4^{2-}, NO_3^{-}, Cl^{-}, and CH_3COO^{-}) with SC were compared (Table 3). Experimental K_{IE} of SO_4^{2-}, NO_3^{-}, and HPO_4^{2-} were close to the calculated constants while K_{IE} for Cl^{-} and CH_3COO^{-} were too low to be evaluated experimentally. The results show the following anion affinity for SC: $HPO_4^{2-} > SO_4^{2-} > NO_3^{-} > Cl^{-} \approx CH_3COO^{-}$, indicating that the SC has the highest affinity for the P anion.

In the case of SC-IE of HPO_4^{2-} and SO_4^{2-}, CO_3^{2-} is liberated in almost equivalent amounts as HPO_4^{2-} is exchanged. The experimental K_{IE} and [SC-IE] were used and a 1:1 exchange was considered in the hydrogeochemical model for HPO_4^{2-}:SO_4^{2-} and 1:2 for the rest of the anions (Table 4).

Model validation with experimental results

For the validation of the model, simulated and experimental results for HPO_4^{2-} and SO_4^{2-} were compared for different SC concentrations (Fig. 1), where a simulated/experimental value of 1 indicates that modeled and experimental results are equal, values above 1 indicate overestimated, and values below 1 indicate underestimated modeled anion removal and recovery.

It is observed that the model reproduces results for P removal and recovery within the experimental error range, especially for lower SC concentrations (Fig. 1a). According to Yuan et al. (2015), at higher concentrations of carbonate (over 30 mM), this may partially dissolve, resulting in increased aqueous cation concentrations that may precipitate with HPO_4^{2}, increasing the P removal. The modeled results

Table 3 Ion exchange equilibrium constants and site concentrations for different anions with the solid carbonate

Anion	[SC-IE] (sites nm^{-2})	Exchanged anion:liberated CO_3^{2-} (eq/eq)	pH	Log K_{IE}		R^2
				Experimental	Calculated[a]	
Cl^{-}	B/D	B/D	9.8 ± 0.1	N/A	− 5	B/D
NO_3^{-}	3.5 ± 0.6	B/D	9.7 ± 0.9	0.5 ± 0.01	0.5	0.99
SO_4^{2-}	4.7 ± 0.7	1.05 ± 0.08	10.4 ± 0.5	0.6 ± 0.06	0.7	0.98
HPO_4^{2-}	4.7 ± 0.5	0.9 ± 0.3	8.8 ± 0.7	1.7 ± 0.05	1.7	0.99
CH_3COO^{-}	B/D	B/D	8.3 ± 0.1	N/A	− 4.5	B/D

B/D ratio could not be determined because CO_3^{2-} was below the detection limit, *N/A* not available because the exchanged anion:liberated CO_3^{2-} ratio could not be determined

[a] Based on ΔG values reported by Drever (1982)

Table 4 Ion exchange reactions and equilibrium constants used in the hydrogeochemical modeling

Exchanged anion	Equation	Log(K_{IE})
HPO_4^{2-}	SC-IE-CO_3 + HPO_4^{2-} ⇄ SC-IE-HPO_4 + CO_3^{2-}	1.7[a]
SO_4^{2-}	SC-IE-CO_3 + SO_4^{2-} ⇄ SC-IE-SO_4 + CO_3^{2-}	0.6[a]
NO_3^-	SC-IE-CO_3 + $2NO_3^-$ ⇄ SC-IE-$(NO_3)_2$ + CO_3^{2-}	0.5[a]
Cl^-	SC-IE-CO_3 + $2Cl^-$ ⇄ SC-IE-$(Cl)_2$ + CO_3^{2-}	− 5.0[b]
CH_3COO^-	SC-IE-CO_3 + $2CH_3COO^-$ ⇄ SC-IE-$(CH_3COO)_2$ + CO_3^{2-}	− 4.5[b]

[a] This study

[b] Calculated with ΔG values reported by Drever (1982)

indicate that P removal by precipitation did not occur even in the absence of SC at the modeled concentrations.

In the case of SO_4^{2-}, the model reproduces experimental results of P removal, with a slight underestimation for [SC-IE] higher than 1, but within the experimental error ranges (Fig. 1b). The model also reproduces the experimental recovery results within the error ranges.

Overall, the validation of the model with the experimental data establishes that the simulated results can describe the HPO_4^2 and SO_4^{2-} removal processes with errors below 5% and HPO_4^2 and SO_4^{2-} recovery processes with errors below 10% of experimental results.

Simulation of phosphorus removal and recovery in biodigestor-treated swine effluent

The simulations of SC-IE of HPO_4^{2-} for different BTSE compositions (maximum, average, and minimum concentrations of each parameter except pH and alkalinity) are presented in Fig. 2. For the average composition of BTSE, SC-IE removes 50% of HPO_4^{2-}. As HPO_4^{2-} concentrations increase, removal by SC-IE decreases and vice versa. The HPO_4^{2-} removal was not largely affected by variations of the cations Fe^{2+}, Mg^{2+}, and Ca^{2+} and the anion SO_4^{2-}. According to these results, none of the evaluated major ions would have a large effect on the P removal by SC-IE.

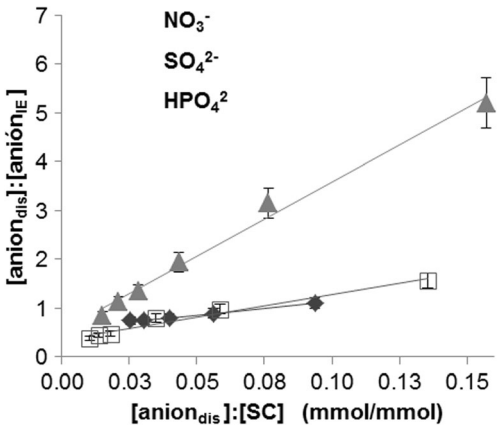

Fig. 1 Comparison of modeled and experimental exchange for different anions

To determine the amount of SC necessary to remove HPO_4^{2-} for the average BTSE composition (Table 1), the ion exchange on SC was simulated for different [SC-IE]:[HPO_4] molar ratio, observing a direct relation of HPO_4^{2-} removal in the whole range of [SC-IE]:[HPO_4] molar ratio between 0.2 and 1.6, and a linear relation between 0.4 and 1.4 (Fig. 3). The most advantageous HPO_4^{2-} removal was obtained when the molar concentration of SC-IE is 1.4 times higher than that of HPO_4^{2-} where a P removal of 92.5% was observed. At the [SC-IE]:[HPO_4^{2-}] molar ratio 1.6, the increase in the removal HPO_4^{2-} deviates from linearity and only 4% extra removal is obtained.

Likewise, to evaluate the amount of CO_3^{2-} required for elution of ion-exchanged HPO_4^{2-} in SC, four different concentrations of Na_2CO_3 were evaluated for different [SC-IE]:[HPO_4] molar ratios (Fig. 4).

It is observed that increasing eluent CO_3^{2-} concentration by one order of magnitude, from 2 to 20 mM Na_2CO_3, an

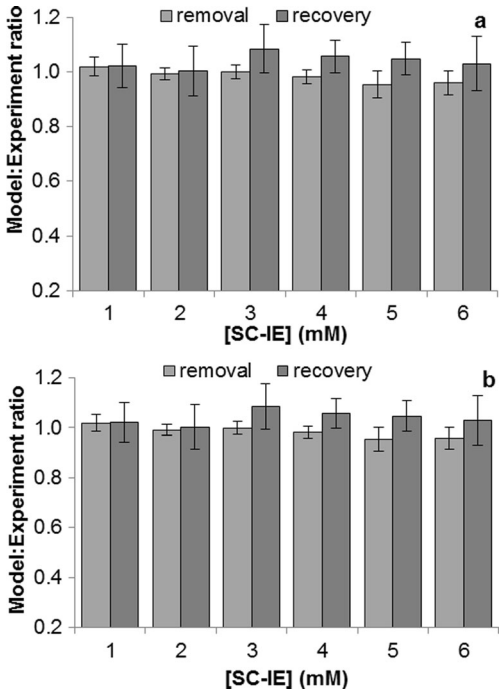

Fig. 2 Model validation of anion removals and recoveries

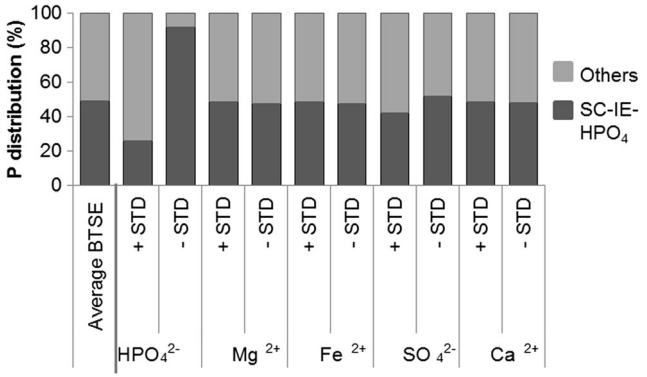

Fig. 3 Simulation of HPO_4^{2-} removal in solid carbonate at different major ion concentrations

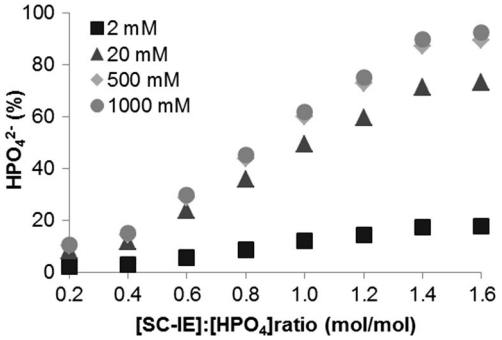

Fig. 5 Simulation of HPO_4^{2-} recovery from solid carbonate with different CO_3^{2-}-eluent concentrations

increase in P recovery of 4.5 is observed for all [SC-IE]:[HPO_4] molar ratio. By increasing the eluent CO_3^{2-} concentration further to 500 mM Na_2CO_3, the amount of recovered P is increased five times with respect to the lowest eluent concentration of 2 mM. Finally, by increasing the eluent concentration to 1000 mM, the five times increase in the amount of recovered HPO_4^{2-} remains almost the same as for the eluent concentration of 500 mM, suggesting that an eluent CO_3^{2-} concentration higher than 500 mM does not represent a significant advantage in the P recovery.

Overall, the results suggest that it is possible to recover 90% of the initial HPO_4^{2-} using a [SC-IE]:[HPO_4] molar ratio of 1.4 and Na_2CO_3 of 500 mM. Under these conditions, 92.5% P is removed and 90% of removed P is recovered, 7.5% of initial HPO_4^{2-} would be discharged, and 2.5% would continue to be attached to the SC, because it is not possible to fully regenerate this material. In addition, the recovery efficiency may vary after various process cycles, although this remains to be evaluated.

The speciation of SC-IE shows that HPO_4^{2-} occupy approximately 60% of the surface sites at average BTSE and that, depending on the HPO_4^{2-} concentration, this may vary between 30 and 80% (Fig. 5). The remaining surface sites are mainly occupied by CO_3^{2-}, HCO_3^-, and, to a much lesser extent, by SO_4^2. Other anions in BTSE, such as CH_3COO^- and Cl^-, do not appear to compete with HPO_4^{2-} for the SC-IE, probably because the affinity is too low (Table 3; Fig. 6).

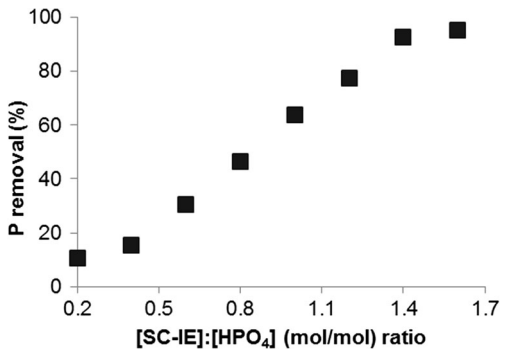

Fig. 4 Simulation of HPO_4^{2-} removal from biodigestor-treated swine effluent on solid carbonate

In order to evaluate the effect of the CO_3^{2-} in the removal of HPO_4^{2-} with SC, the relations between SC-IE and alkalinity and between alkalinity and HPO_4 were modeled for the average BTSE composition (Table 1). Increasing the SC concentration nine-fold (increasing [SC-IE]:[alkalinity] molar ratio from 0.1 to 0.9) HPO_4^{2-} is more readily removed and recovered (Fig. 7a). On the other hand, increasing the [alkalinity]:[HPO_4] molar ratio from 2.5 to 25, or increasing alkalinity ten-fold, both HPO_4^{2-} removal and recovery decrease.

The [SC-IE]:[alkalinity] molar ratio of 0.57 represents the most convenient ratio for recovery of P (Fig. 7a). At this ratio, almost one-third of SC-IE are occupied by CO_3^{2-} and the remaining sites with HPO_4^{2-} (Fig. 5). To increase P removal under conditions of average BTSE, [SC-IE] should be increased.

On the other hand, the [alkalinity]:[HPO_4] molar ratio of 12, which is found in average BTSE, allows the removal 60% of HPO_4^{2-}, and it is feasible to obtain 99% of P removal at [alkalinity]:[HPO_4] molar ratio of 2.5. The P removal by SC-IE is reduced as the [alkalinity]:[HPO_4] molar ratio is increased. In order to improve the P removal and recovery by SC-IE, reducing the quantity of alkalinity-CO_3^{2-} in the system, allows reducing the competition between HPO_4^{2-} and CO_3^2 for SC-IE. However, the process typically used to reduce CO_3^{2-} in water such as inverse osmosis, are not likely to work in BTSE due to high concentrations of suspended solids (Crittenden et al. 2012). Alkalinity may also be reduced by acidification causing the removal of CO_2 or by precipitation of $CaCO_3$. However, this is not a feasible option for BTSE and either would also interfere with SC-IE. Therefore, to increase P removal in BTSE [SC-IE] should most conveniently be increased.

Comparison between phosphorus removal methods

The SC-IE method for HPO_4^{2-} removal in BTSE was compared with two other methods commonly used for HPO_4^{2-} removal in swine effluents: struvite precipitation and application of aluminum sulfate (Fig. 8).

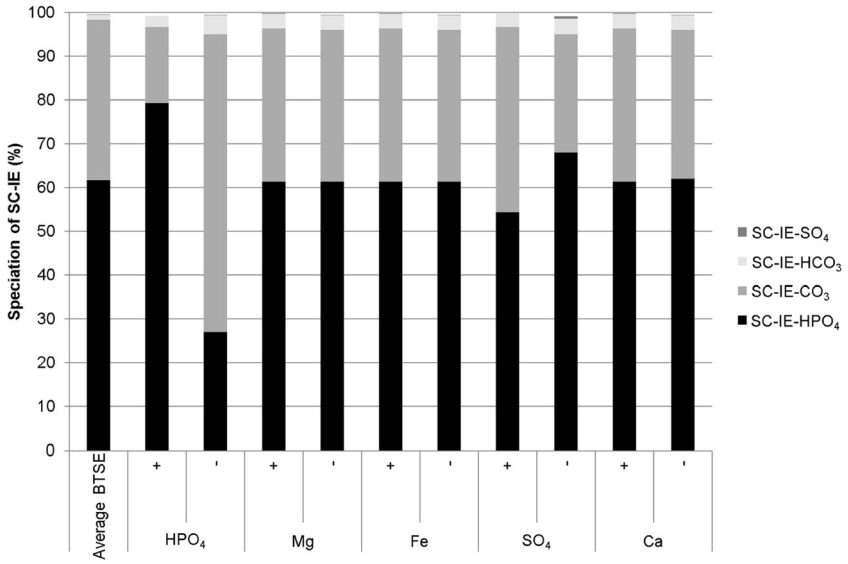

Fig. 6 Ion exchange site speciation after HPO_4^{2-} removal from biodigestor-treated swine effluent on solid carbonate

The results suggest that struvite precipitation is highly dependent on pH being P removal most efficient around pH 10. At the pH of BTSE, a P removal between 50 and 100 mg l^{-1} is observed (from 350 to between 300 and 250 mg l^{-1}). Likewise, P removal by application of $Al_2(SO_4)_3$ is strongly pH dependent (Fig. 7). Therefore, to remove P using this method, it is necessary to reduce pH to between 4.7 and 6.2 where 50% P removal is estimated (from 350 to 175 mg l^{-1}). The ion exchange with SC was analyzed using two different [SC-IE]:[HPO_4] molar ratios, 0.8 and 1.4. With a [SC-IE]:[HPO_4] molar ratio of 1.4, the SC method shows between 90 and 100% removal of P in the pH range of BTSE. SC is affected by pH because it is expected to dissolve at pH below 6.9 where carbonate is expected to dissolve, and above 7.7 where the cation forms hydroxides. However, among the evaluated methods, IE SC appears to be the most effective for P removal at the pH range of BTSE. This method would allow not only obtaining P concentrations below maximum allowable limits but also being able to recover the nutrient as inorganic P that may be reused in agricultural and industrial applications to mitigate a P-scarce future.

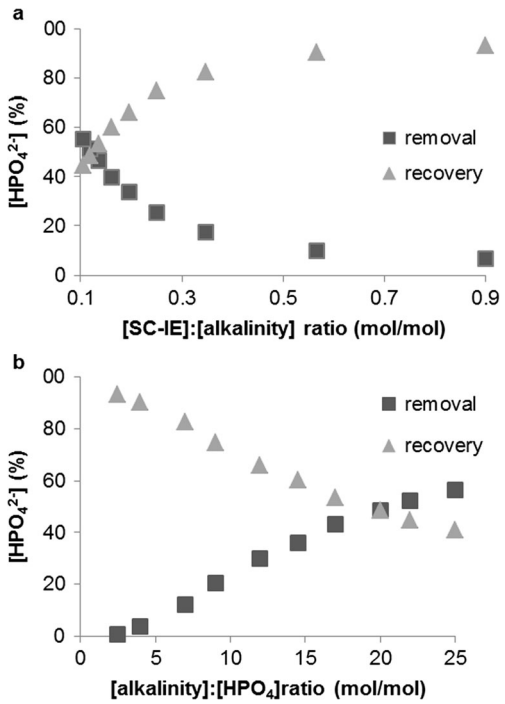

Fig. 7 Dissolved HPO_4^{2-} removal and recovery as a function of **a** [SC-IE]:[alkalinity] molar ratio and **b** [alkalinity]:[HPO_4] molar ratio. + STD and − STD indicate maximum and minimum modeled concentrations

Conclusions

Different methods to remove P from BTSE were compared by hydrogeochemical modeling: SC-IE, application of $Al_2(SO_4)_3$, and struvite precipitation. At pH ranges usually found in BTSE, SC-IE was found to be the most efficient method to remove inorganic P and allowing discharges to comply with regulation levels.

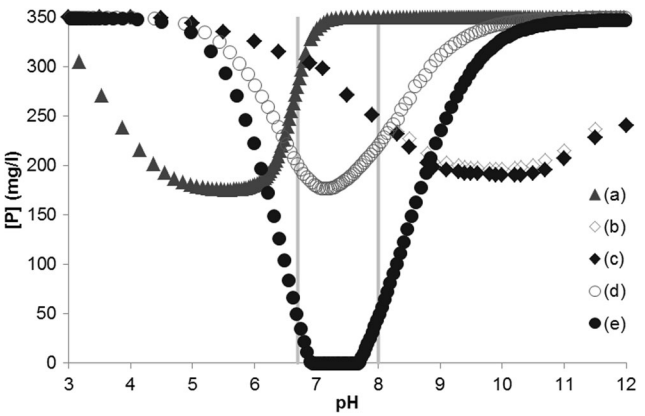

Fig. 8 Comparison of different methods for HPO_4^{2-} removal

Phosphorus removal and recovery from BTSE with SC was also evaluated by hydrogeochemical modeling, with thermodynamic data obtained from the literature except K_{IE} and [SC-IE] for different anions in BTSE that were obtained experimentally. The mechanisms for P removal and recovery by SC-IE were evaluated by thermodynamic description of the different reactions involved in the process. The simulation of the SC-IE process for different ion concentrations in BTSE showed a strong effect of alkalinity on P removal. After the P removal by ion exchange in BTSE, 60% of the SC-IE sites were replaced with HPO_4^{2-}, close to 40% with CO_3^{2-} while SO_4^{2-} exchanged with only 1% of the SC-IE sites. To reduce the effect of high alkalinity s in BTSE for P removal by ion exchange, [SC-IE] should be increased. Simulations of the SC-IE recovery allowed retrieving 90% P retrieval by eluting with 500 mM CO_3^2, or 142:1 (molar ratio) CO_3^{2-} for each recovered HPO_4^{2-}, since the latter is bound very strongly to SC-IE.

The results suggest that SC-IE may be effective for P removal and recovery in average concentrations of BTSE, offering a method to reduce discharges of P that otherwise produce eutrophication, and thereby protecting water bodies. Besides, SC-IE may recover inorganic P that can be reused in agricultural or industrial processes, mitigating the upcoming P scarcity.

Acknowledgments The authors thank Simón González and Georgina Izquierdo for their advice during this study, as well as Axel Falcón, Gonzalo Jayme, and Carlos Corzo for their support during this work.

Funding information This work was supported by the Mexican Institute of Water Technology (Project numbers TH1505 and TH1606. The Mexican National Council for Science and Technology (CONACYT) provided a doctoral scholarship for Luis Cueto (scholarship number 394206).

References

Barker JC, Overcash MR (2007) Swine waste characterization: a review. Transactions of the ASABE 50(2):651–657. https://doi.org/10.13031/2013.22654

Bergland WH, Dinamarca C, Toradzadegan M, Nordgård ASR, Bakke I, Bakke R (2015) High rate manure supernatant digestion. Water Res 76:1–9. https://doi.org/10.1016/j.watres.2015.02.051

Blanc P. (2017) – Thermoddem : Update for the 2017 version. Report BRGM/RP-66811-FR, 20 p. http://thermoddem.brgm.fr/sites/default/files/upload/documents/brgmrp-66811-fr_final_report.pdf. Accessed Abril 22, 2019

Cheng, J., M. M. Peet, and D. H. Willits. (2003) Ambient temperature anaerobic digester and greenhouse for swine waste treatment and bioresource recovery at Barham farm. Proceedings of the 2003 North Carolina Animal Waste Management Workshop, October 16-17, 2003, Durham, NC, USA.

Cordell D, Rosemarin A, Schröder JJ, Smit AL (2011) Towards global phosphorus security: a systems framework for phosphorus recovery and reuse options. Chemosphere 84(6):747–758. https://doi.org/10.1016/j.chemosphere.2011.02.032

Crittenden JC, Trussell RR, Hand DW, Howe KJ, Tchobanoglous G (2012) MWH's water treatment: principles and design. John Wiley and Sons, Hoboken. https://doi.org/10.1002/9781118131473

Cueto LA, Hansen AM (2017) Synthesis and characterization of ion exchangers for phosphorus control in water. In: Hernández-Bárcenas LG, Mendoza-Chávez YJ, Martínez-Villegas N (eds) Actas INAGEQ., vol 23, pp 301–309 (in Spanish)

Drever JI (1982) The geochemistry of natural waters. Prentice-Hall, Englewood Cliffs. https://doi.org/10.1029/97EO00305

Jayme-Torres G, Hansen AM (2018) Nutrient loads in the river mouth of the Río Verde basin in Jalisco, Mexico: how to prevent eutrophication in the future reservoir. Environ Sci Pollut Res Int 2018(25):20497–20509. https://doi.org/10.1007/s11356-017-0334-2

LLNL (Lawrence Livermore National Laboratory) (2010) llnl.dat. http://www.phreeplot.org/ppihtml/llnl.dat.html. Accessed August 23 2018

Martin JH (2003) An Assessment of the Performance of the Colorado Pork, LLC. Anaerobic Digestion and Biogas Utilization System, Report 03-007, Biogas Recovery in the Agriculture Sector State of Colorado Governor's Office Of Energy Management and Conservation; Colorado, 39 p. http://agrienvarchive.ca/bioenergy/download/CP_Report_Colorado_v2_2003.pdf. Assessed April 22, 2019

Meers E, Rosseau DPL, Lesage E, Demeersseman E, Tack F (2006) Physico-chemical P removal from the liquid fraction of pig manure as an intermediary step in manure processing. Water Air Soil Pollut 169(1):317–330. https://doi.org/10.1007/s11270-006-3112-1

Mehta CM, Batstone DJ (2013) Nutrient solubilization and its availability following anaerobic digestion. Water Sci Technol 67(4):756–763. https://doi.org/10.2166/wst.2012.622

Parkhurst DL, Appelo CAJ. (2013) Description of Input and Examples for PHREEQC Version 3—A Computer Program for Speciation, Batch-Reaction, One-Dimensional Transport, and Inverse Geochemical Calculations. US Geological Survey Techniques and Methods, Book 6, Chapter A43, 497 p. http://pubs.usgs.gov/tm/06/a43. Accessed August 23 2018

Ra CS, Lo KV, Shin JS, Oh JS, Hong BJ (2000) Biological nutrient removal with an internal organic carbon source in piggery wastewater treatment. Water Res 34(3):965–973. https://doi.org/10.1016/S0043-1354(99)00189-X

Rittmann BE, Mayer B, Westerhoff P, Edwards M (2011) Capturing the lost phosphorus. Chemosphere 84(6):846–853. https://doi.org/10.1016/j.chemosphere.2011.02.001

Rodríguez A, Lomas J (1999) Transition of particle size fractions in anaerobic digestion of the solid fraction of piggery manure. Biomass Bioenergy 17(5):229–235. https://doi.org/10.1016/S0961-9534(99)00059-8

Suzuki K, Tanaka Y, Kuroda K, Hanajima D, Fukumoto Y, Yasuda T, Waki M (2007) Removal and recovery of phosphorous from swine wastewater by demonstration crystallization reactor and struvite accumulation device. Bioresour Technol 98(8):1573–1578. https://doi.org/10.1016/j.biortech.2006.06.008

Türker M, Erdem İÇ (2011) Chemical equilibrium model of struvite precipitation from anaerobic digester effluents. Turk J Eng Environ Sci 35(1):39–48. https://doi.org/10.3906/muh-1008-15

Van den Berg CMG, Kramer JR (1979) Determination of complexing capacities of ligands in natural waters and conditional stability constants of the copper complexes by means of manganese dioxide. Anal Chim Acta 106(1):113–120. https://doi.org/10.1016/S0003-2670(01)83711-9

Wagman DD, Evans WH, Parker VB, Schumm RH, Halow I (1982) The NBS tables of chemical thermodynamic properties. National Standard Reference Data System, Gaithersburg. https://doi.org/10.1063/1.555845

Xu N, Li Y, Zheng L, Gao Y, Yin H, Zhao J, Chen M (2014) Synthesis and application of magnesium amorphous calcium carbonate for

removal of high concentration of phosphate. Chem Eng J 251:102–110. https://doi.org/10.1016/j.cej.2014.04.037

Ye ZL, Chen SH, Lu M, Shi JW, Lin LF, Wang SM (2011) Recovering phosphorus as struvite from the digested swine wastewater with bittern as a magnesium source. Water Sci Technol 64(2):334–340. https://doi.org/10.2166/wst.2011.720

Yuan X, Xia W, An J, Yin J, Zhou X, Yang W (2015) Kinetic and thermodynamic studies on the phosphate adsorption removal by dolomite mineral. J Chem 2015:1-8 https://www.hindawi.com/journals/jchem/2015/853105/. Accessed August 23 2018 https://doi.org/10.1155/2015/853105